Calcium extrusion is critical for cardiac morphogenesis and rhythm in embryonic zebrafish hearts

A. M. Ebert*[†], G. L. Hume*[†], K. S. Warren[‡][§], N. P. Cook*, C. G. Burns[‡], M. A. Mohideen[‡], G. Siegal[¶], D. Yelon[¶], M. C. Fishman[‡][‖], and D. M. Garrity*[‡]**

*Department of Biology, Colorado State University, Fort Collins, CO 80523; [‡]Cardiovascular Research Center, Massachusetts General Hospital, Harvard Medical School, Charlestown, MA 02129; and [¶]Developmental Genetics Program, Skirball Institute of Biomolecular Medicine, New York University School of Medicine, New York, NY 10016

Calcium entry into myocytes drives contraction of the embryonic heart. To prepare for the next contraction, myocytes must extrude calcium from intracellular space via the Na$^+$/Ca^{2+} exchanger (NCX1) or sequester it into the sarcoplasmic reticulum, via the sarcoplasmic reticulum Ca^{2+}-ATPase2 (SERCA2). In mammals, defective calcium extrusion correlates with increased intracellular calcium levels and may be relevant to heart failure and sarcoplasmic dysfunction in adults. We report here that mutation of the cardiac-specific NCX1 (*NCX1h*) gene causes embryonic lethal cardiac arrhythmia in zebrafish *tremblor* (*tre*) embryos. The *tre* ventricle is nearly silent, whereas the atrium manifests a variety of arrhythmias including fibrillation. Calcium extrusion defects in *tre* mutants correlate with severe disruptions in sarcomere assembly, whereas mutations in the L-type calcium channel that abort calcium entry do not produce this phenotype. Knockdown of *SERCA2* activity by morpholino-mediated translational inhibition or pharmacological inhibition causes embryonic lethality due to defects in cardiac contractility and morphology but, in contrast to *tre* mutation, does not produce arrhythmia. Analysis of intracellular calcium levels indicates that homozygous *tre* embryos develop calcium overload, which may contribute to the degeneration of cardiac function in this mutant. Thus, the inhibition of NCX1h versus SERCA2 activity differentially affects the pathophysiology of rhythm in the developing heart and suggests that relative levels of NCX1 and SERCA2 function are essential for normal development.

heart development | arrhythmia | sodium calcium exchanger | Ca^{2+}-ATPase

Rhythm in the embryonic heart is progressively acquired. Peristaltic contractions in the heart tube gradually give way to synchronized beats as the atrium and ventricle differentiate (1, 2). Arrhythmias are associated with pathological conditions in neonates and adults (3), and animal models are required to fully understand the normal and abnormal manifestation of rhythms early in cardiac development. We identified the zebrafish cardiac arrhythmia mutant *tremblor* (*tre*) in a genetic screen for cardiac defects causing embryonic lethality.

In cardiac myocytes, intracellular calcium concentrations are stringently controlled because of the intimate role this ion plays in myofilament contraction. Regulation of the heartbeat requires variation in calcium concentrations during relaxation and contraction. To facilitate relaxation, two calcium regulatory proteins, the sodium calcium exchanger (NCX1) and sarcoplasmic reticulum (SR) Ca^{2+}-ATPase2 (SERCA2), orchestrate the extrusion of calcium across the sarcolemma or its sequestration into the SR, respectively. Na$^+$/Ca^{2+} exchangers regulate the intracellular Ca^{2+} concentration in cells in response to the prevailing electrochemical gradient and catalyze the exchange of three extracellular Na$^+$ ions for one intracellular Ca^{2+} ion (4, 5). In mammals, *NCX1* activity is the dominant mechanism for extrusion of Ca^{2+} from intracellular space, which is necessary for

the cardiomyocyte to return to the resting state after excitation (6). The SERCA Ca^{2+}-ATPase is an intracellular pump located in the SR or endoplasmic reticula of muscle cells. The *SERCA2a* isoform plays a central role in excitation–contraction coupling in the heart, where it pumps Ca^{2+} back into the SR to replenish the stores needed for the next contraction (7).

The relative contributions of NCX1 and SERCA2 to calcium modulation in the heart vary by species, by developmental stage, and in some cases by region of the heart (8–11). In mouse, SR is scarce in immature cardiomyocytes at the electron-microscope level, suggesting that Na$^+$/Ca^{2+}-exchange may constitute the more prevalent mechanism for modulating calcium in immature myocytes (10). Consistent with this hypothesis, mouse *SERCA2* is expressed only at low levels in the embryonic heart field but increases 8-fold by adulthood, whereas *NCX1* is 2-fold higher in fetal tissues than adult (9). The embryonic dependence on NCX1 is not absolute, however, because targeted mutation of either gene is embryonic lethal (12–14).

Unlike the mouse, the zebrafish embryo can survive for 1–2 days even in the absence of a heartbeat, living by diffusion of oxygen from the surrounding water. Thus, zebrafish models make it feasible to track the functional effects of molecular deficiencies in calcium-handling genes.

Materials and Methods

See *Supporting Text*, which is published as supporting information on the PNAS web site, for additional methods on positional cloning, RACE, *in situ* hybridization, and electron microscopy. The SERCA2 *in situ* probe was made from IMAGE clone 2601981 (GenBank accession no. BC045327.1).

Morpholino or Pharmacological Inhibition and Phenotypic Rescue. The morpholino-modified antisense oligonucleotide (Gene-Tools, Corvallis, OR) MO1 (5′-TGTTCCCAGTGAGG-TATTTTGTTCC-3′) targets −24 to +1 of the cardiac-specific sodium calcium exchanger 1 (*NCX1h*) coding region. MO2 (5′-GGAAGAGAATCCCGCTCAAGTCAAG-3′) targets −34
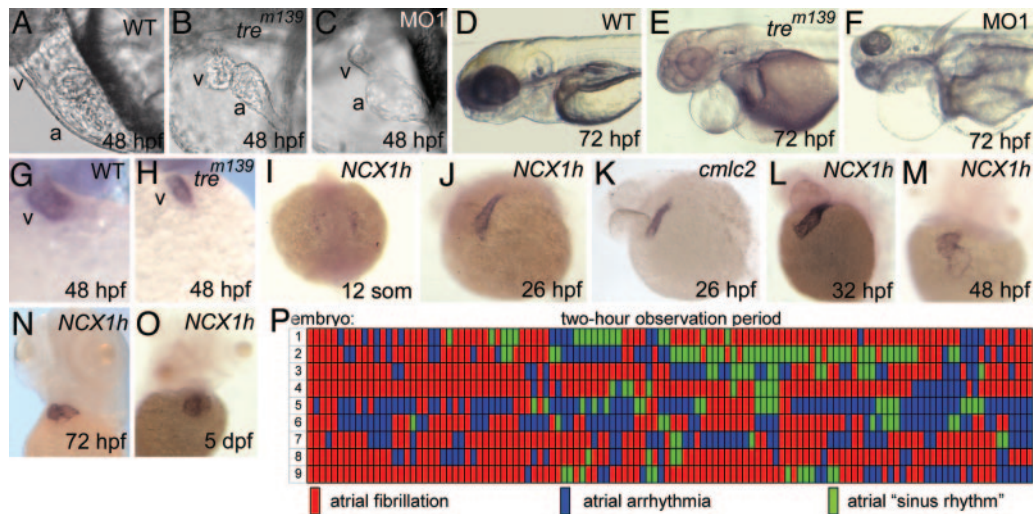
Fig. 1. Cardiac defects in homozygous *tre* embryos. (*A* and *B*) Cardiac development at 48 hpf. The ventricle of *tre* mutants (*B*) is small and collapsed. (*C*) Injection of *NCX1h*-morpholino (MO1) phenocopies *tre*. (*D–F*) At 72 hpf, *tre* mutants and morphants show pericardial edema and slightly smaller heads. Heterozygous *tre* embryos (not shown) have no overt phenotype. (*G* and *H*) By 48 hpf, the ventricle, denoted by ventricle-specific *vmhc* expression, is markedly smaller in *tre* mutants. (*I–O*) *NCX1h* expression by *in situ* hybridization. (*I*) *NCX1h* is first detected in bilateral cardiac precursors at the 12-somite stage. (*J* and *K*) At 26 hpf, *NCX1h* expression in the heart tube is similar to *cmlc2*. *NCX1h* expression remains restricted to the heart at (*L*) 32 hpf, (*M*) 48 hpf, (*N*) 72 hpf, and (*O*) 5 days postfertilization. A second zebrafish *NCX1* gene (*NCX1b*) is not expressed in the heart at any stage but is expressed in brain [see Langenbacher *et al.* (32)]. (*P*) Rhythm in the atria of nine *tre* embryos at 48 hpf depicted graphically. Each segment represents a 1-min observation period in which the atrial rhythm was visually scored in a single mutant embryo. Wild-type sibling embryos remained in sinus rhythm throughout the entire testing period (data not shown). No reproducible patterns in rhythm are observed on day 2 (*P*) or 3 (not shown) or in two other experimental replicates. a, atrium; v, ventricle.

to −10 of the *SERCA2* coding region. MO1, MO2, or control morpholino was injected into one to four cell embryos. For pharmacological studies, 24-hr postfertilization (hpf) embryos with chorion intact were exposed to 1–5 μM cyclopiazonic acid (CPA) diluted in egg water from a 20 mM stock in DMSO and scored phenotypically at 48 and 72 hpf. DMSO-treated control embryos developed normally. For rescue, capped mRNAs were synthesized by using the mMessage mMachine kit (Ambion, Austin, TX).

Video Recording and Calcium Imaging. Phase videos of wild-type and *tre* mutant hearts were recorded at 30 or 125 frames per second by using a Photron FASTCAM PCI camera mounted on a Zeiss Axioskop microscope. Calcium orange AM (Invitrogen, C-3015) was dissolved in 0.2 M KCl to 3.5 μM and injected beneath the pericardium of 48-hpf embryos. Surrounding cells (mostly cardiomyocytes) take up the dye because of its acetoxymeythl (AM) derivative. Nonspecific intracellular esterases cleave the AM group to trap the dye inside the cell. Dye-injected embryos were imaged with a Nikon digital camera on a Nikon Eclipse TE2000-4 inverted fluorescent microscope. Videos were compiled by using METAMORPH (Molecular Devices) and IMAGE J (National Institutes of Health, Bethesda) software.

Results and Discussion

We isolated five alleles of the *tre* heart function mutant in ethylnitrosourea-based large-scale genetic screens. In zebrafish, external fertilization and diffusion-mediated oxygen acquisition facilitate the observation of the onset of cardiac rhythm in nonhypoxic embryos over developmental time. Cardiac function is abnormal in homozygous *tre* embryos from the very onset of contraction. In the nascent heart tube at 26 hpf, the presumptive atrial cells actively fibrillate, whereas the presumptive ventricular cells show no overt contraction. Ventricular cardiomyocytes never show coordinated contraction of the chamber and fibrillate only slightly in the first 2 days of development. By 48 hpf, the ventricular chamber is collapsed, distorted, and smaller than wild type (Fig. 1 *A*, *B*, *G*, and *H*). Circulation is never established, and

pericardial edema is prevalent by 72 hpf (Fig. 1 *D* and *E*). In contrast to the ventricle, the atrium of *tre* mutants contracts actively and continuously throughout the first several days of development, cycling through three modes: fibrillation, arrhythmia, and weakly contractile "sinus rhythm" (see Movies 1–4, which are published as supporting information on the PNAS web site). Fibrillating cardiomyocytes contract in a sporadic independent fashion, with no global contraction of the chamber. During arrhythmia, the atrium contracts with a variety of abnormal patterns, including spurts of bradycardia or tachycardia, contractions initiating midatrium that travel backward toward the venous end of the atrium, and double beats of the venous end of the atrial chamber relative to the single beats of the arterial end. In "sinus rhythm," chamber-wide coordinated contractions occur, but contractility is severely diminished. Embryonic lethality occurs at ≈6 days postfertilization.

To search for patterns in atrial rhythm, we tracked hearts of 48 hpf *tre* embryos for 2-hr periods (Fig. 1*P*). Although all embryos cycle through all modes of rhythm, the duration and sequence of each mode are different in every embryo. Variability of *tre* atrial rhythms appears to be stochastic. Arrhythmic phenotypes of the sort reported here, including fibrillation, spells of tachycardia or bradycardia, or cyclic rhythmic behaviors, are not described in any of the *NCX1*-deficient mouse models (13–15) or in studies with NCX-inhibitory compounds (16). The difference in rhythm phenotypes could reflect species differences, or that rhythm is more easily followed in live zebrafish embryos.

We genetically mapped *tre* to a ≈1.0-cM interval on LG11. A chromosomal walk defined contigs within the critical interval containing sequences homologous to mammalian *NCX1* (Fig. 2*A*). The zebrafish genome encodes two *NCX1* genes, named for their heart- (*NCX1h*) or brain-specific (*NCX1b*) expression. On LG11, zebrafish *NCX1h* spans 10 exons and encodes a predicted protein of 969 amino acids that is 74% identical to human *NCX1* (Fig. 2*B*). Sequence homology predicts zebrafish *NCX1h* topology is similar to mammalian models (Fig. 2*E*) (17). RT-PCR with gene-specific primers spanning exons 3–8 produces multiple
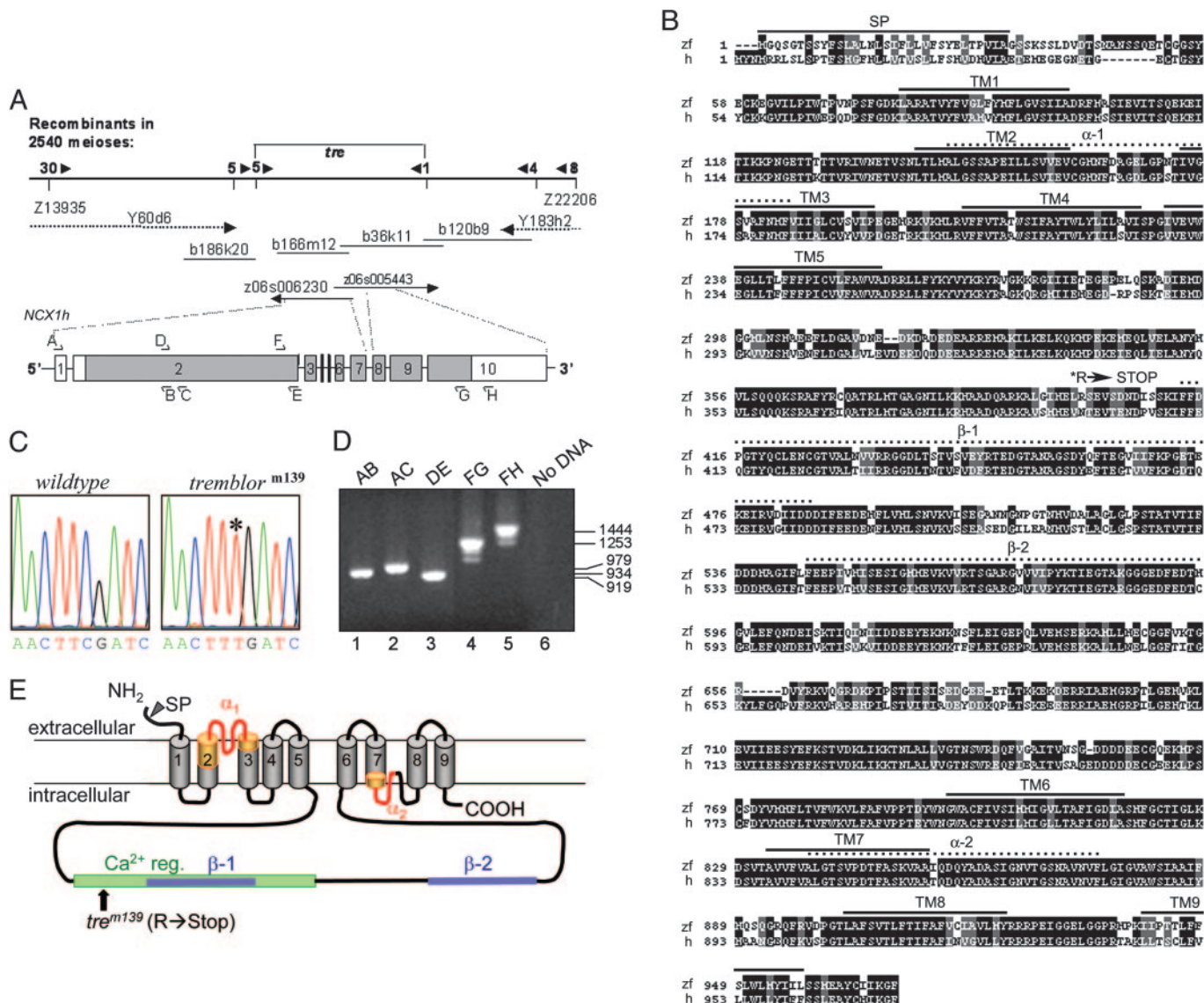
Fig. 2. Zebrafish *tre* encodes an *NCX1* gene. (*A*) An integrated physical and genetic map of the *tre* locus, showing selected polymorphic microsatellite markers (''Z markers'') and the number of recombinant events detected from 2540 meiosis. Two genomic contigs (z06s006230 and z06s005443) contain sequences homologous to mammalian NCX1. The 3,052-bp zebrafish *NCX1h* (GenBank accession no. AY937230) ORF includes a noncoding first exon and a large second exon that comprises ≈60% of the coding sequence. The *NCX1h* genomic sequence extends over ≈74,000 kb. Introns not drawn to scale. (*B*) Alignment of zebrafish and human NCX1 (GenBank accession no. NP_066920.1). Topological domains include nine highly conserved transmembrane (TM) segments, α-1 and α-2 repeat motifs characteristic of all exchangers in the cation/Ca^{2+} superfamily (33) (PFAM01699), and β-1 and β-2 CalX domains found in Na^+/Ca^{2+} exchangers and integrin subunit β4 (GenBank accession no. PFAM03160) (33). Black boxes, amino acid identity; gray boxes, conserved substitutions; *, site of *tre^{m139}* mutation; SP, predicted signal peptide domain. (*C*) Sequencing of *NCX1h* cDNA reveals a C to T nucleotide transition at codon 400 (CGA→TGA) in *tre^{m139}* mutant embryos. (*D*) RT-PCR analysis of *NCX1h* is consistent with alternative splicing in exons three-prime to exon 2. Sequencing of products defines five isoforms that vary in the combinations of several small exons that comprise the large intracellular loop (D.M.G., unpublished work). Lanes are labeled with primers used (see *A* for primer locations). Lanes 1–3, single bands are amplified by using primers that span exons 1 and 2; lanes 4 and 5, multiple products (suggesting multiple isoforms) are obtained by RT-PCR by using primers that span exons 2–10; lane 6, no DNA control. (*E*) Predicted topology for zebrafish NCX1h is similar to mammalian models, including five N- and four C-terminal transmembrane domains (cylinders) separated by a large cytoplasmic loop responsible for regulation of exchange activity (34, 35).

products, suggesting alternative splicing occurs in the same region as mammalian isoforms (Fig. 2*D*).

The *tre^{m139}* allele contains a C to T nucleotide transition at codon 400 (CGA→TGA) of *NCX1h*. Replacement of an arginine codon by a stop codon is predicted to cause premature termination of NCX1h in the cytoplasmic loop shortly after transmembrane domain 5 (Fig. 2 *C* and *E*). Truncation of NCX1h in *tre^{m139}* should abrogate or severely reduce its activity by eliminating the Ca^{2+} regulatory domain, four carboxyl trans-

membrane segments, and the α-2 domain shown in human *NCX1* to be essential for a functional exchanger (18). No functional activity was observed in analogous mutations in mammalian *NCX1* that truncate the exchanger to the first five transmembrane domains plus varying lengths of cytoplasmic loop (19). To confirm that *tre* defects are due to loss of *NCX1h* function, we reduced NCX1h levels by injection of a morpholino-modified antisense oligonucleotide (MO1) directed against the *NCX1h* translational start site. Approximately 95% of embryos injected

GENETICS

with 2 ng of MO1 reproduce the *tre* mutant phenotype (Fig. 1 *A–F*; see also Table 1, which is published as supporting information on the PNAS web site). Injection of MO1 fails to elicit cardiac phenotypes more severe than homozygous *tre^m139* embryos, supporting the hypothesis that *tre^m139* is a strong loss-of-function allele. Because NCX1 is highly conserved among vertebrates, we tested whether murine NCX1 could rescue cardiac function in homozygous *tre* mutants. We find injection of 200 pg of murine NCX1 RNA partially rescues 33% of homozygous *tre* mutant embryos ($n = 24$), restoring normal size, morphology, and contractility to the ventricle at 48 hpf but not fully rescuing atrial rhythm (Table 2, which is published as supporting information on the PNAS web site). In comparison, injection of zebrafish *NCX1h* RNA at least partially rescued 30% of homozygous *tre* mutant embryos ($n = 33$), including 5% ($n = 6$) fully rescued embryos (Table 2). Thus, zebrafish and mouse *NCX1* proteins share a degree of functional conservation *in vivo*.

The expression pattern of *NCX1h* correlates well with the heart-specific nature of *tre* defects. *NCX1h* expression is first detectable at the 12-somite stage in bilateral populations of cardiac precursors (Fig. 1*I*). The length and morphology of the heart tube are normal in *tre* mutant embryos. Similar to *cardiac myosin light chain 2* (*cmlc2*) expression (20) (Fig. 1 *J* and *K*), *NCX1h* expression is restricted to the heart through at least 5 days postfertilization (Fig. 1 *L–O*). In contrast, the initial cardiac-specific expression of mouse *NCX1* expands later in embryogenesis to include portions of the central nervous system (21). To investigate the specification of cardiac precursors, homozygous *tre* mutant embryos were tested with a panel of cardiac-specific markers. Expression of *ventricular myosin heavy chain* (*vmhc*), *cmlc2*, *tbx5*, and *hand2* (20, 22, 23) is normal at the 15- and 20-somite stage (data not shown), suggesting early cardiac specification and early differentiation are normal in *tre* mutants.

Morphological defects appear as the ventricular and atrial chambers differentiate. In particular, the ventricle is markedly smaller in *tre* mutants (Fig. 1 *G* and *H*). The contractile deficiency of the ventricle in homozygous *tre* mutants may be due to mechanical deficiencies (e.g., sarcomere defects) or to failure of conduction to progress from normal sites in the atrium. We examined sarcomere formation in *tre* mutant embryos by transmission electron microscopy at 48 hpf, by which time multiple consecutive sarcomeres with well-defined Z lines are evident in wild-type embryos (Fig. 3 *A* and *B*). In ventricles of homozygous *tre* mutants, sarcomeres are sparse, randomly orientated, and rarely linked in units of more than two (Fig. 3 *C* and *D*). *tre* mutants do not display marked abnormalities in sarcomere formation in the atrium (Fig. 3 *E–H*). Sarcomere formation in the *island beat* (*isl*) mutant (encoding an L-type calcium channel) was normal (24), suggesting that the *tre* sarcomere assembly defects are not a secondary consequence of functional defects arising from lack of blood flow, poor contractility, or poor ventricle growth. Although both *isl* and *tre* affect calcium handling, defects in calcium extrusion but not calcium entry were associated with myofibrillar abnormalities. We conclude that *NCX1h* is essential for sarcomere formation or maintenance in the embryonic ventricle, potentially via an indirect mechanism.

To determine whether *SERCA2* was likely to play a significant role in early heart function in zebrafish, we examined *SERCA2* expression in heart development. *SERCA2* encodes a predicted protein of 996 amino acids that is 84% identical to human *SERCA2*. Moreover, zebrafish and human *SERCA2* are 75% identical in the first 28 amino acids, a critical region for protein retention in the SR (25). Zebrafish *SERCA2* is expressed robustly in the cardiac precursors, throughout the forming heart, and in skeletal muscle (Fig. 4 *A–F*). Robust cardiac *SERCA2* expression and sequence homology to SR-retention domains
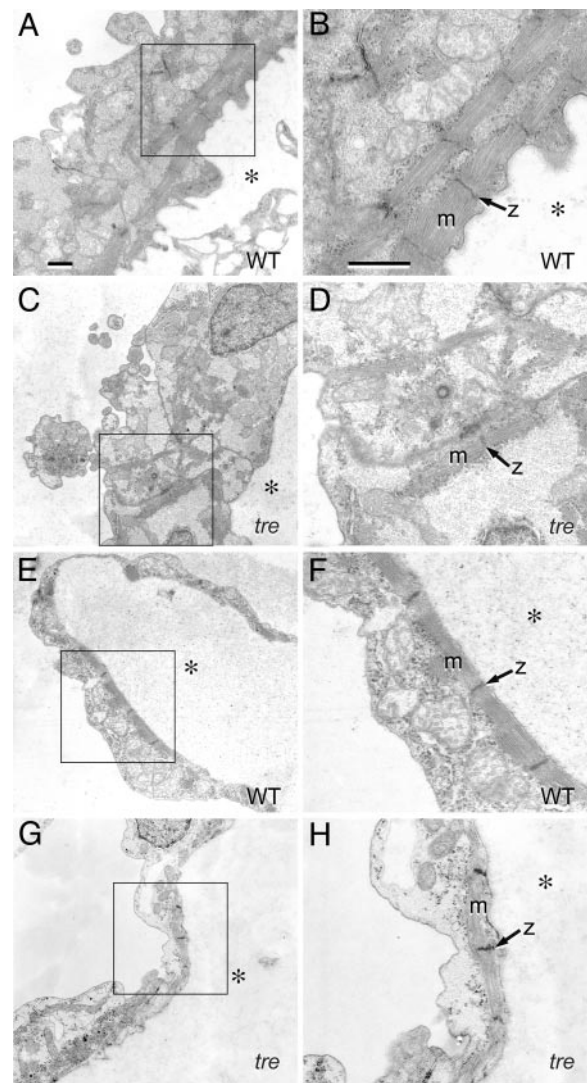

Fig. 3. Mutation of *NCX1h* is associated with myofibrillar defects in the ventricle. Transmission electron micrographs of embryonic hearts at 48 hpf. (*A–D*) Ventricle. In the wild-type ventricle (*A*), myofibrillar arrays are present along the interior aspect of the chamber and (*B*) bundled into consecutive units. In the *tre* ventricle (*C*), sarcomeres are scarce, randomly arrayed, and form few consecutive units. (*D*) Myofibrillar bundles are thin and lack distinct Z lines. (*E–H*) Atrium. In the atrium, both wild-type (*E* and *F*) and *tre* mutants (*G* and *H*) assemble consecutive sarcomeric units on the interior aspect of the chamber, with no substantial defects in *tre* mutants. However, the atrial cytoplasmic space in *tre* mutants (*H*) is electron-lucent, potentially indicative of decreased glycogen accumulation. (Bars, 1 μm.) *B*, *D*, *F*, and *H* are magnifications of boxed regions of *A*, *C*, *E*, and *G*, respectively. Magnification in *A* applies to *C*, *E*, and *G*; magnification in *B* applies to *D*, *F*, and *H*. ∗ denotes the interior of the heart chamber.

suggests significant levels of SR are likely to be present in zebrafish embryonic hearts.

To evaluate the role of SERCA2 in the onset of cardiac rhythm, we reduced zebrafish *SERCA2* function by injection of morpholino directed against the *SERCA2* translational start site (MO2) or by treatment with CPA, a specific inhibitor of SERCA activity (26–28). The cardiac chambers of MO2-injected or CPA-treated embryos fail to expand, and the heart fails to loop (Fig. 4 *L–T* and Table 1). Heart rate is slowed 30–50%, contractility is weak, and circulation is usually absent. In contrast to *tre* mutants, both ventricle and atrium consistently contract, and no fibrillation occurs. Lethality occurs at ≈6 days postfer-
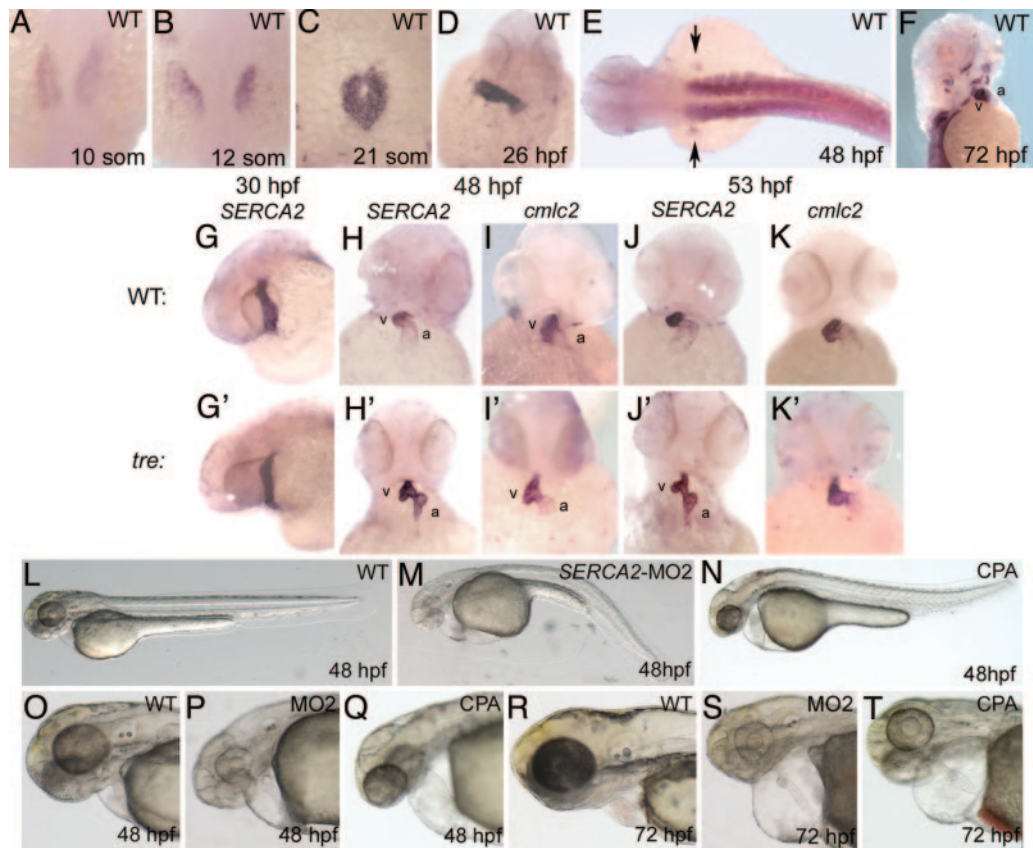
Ebert *et al.*

Fig. 4. *SERCA2* is essential for cardiac development. (*A–F*) *SERCA2* expression in early development. *SERCA2* RNA is expressed in (*A–C*) the bilateral cardiac precursors; (*D*) the heart tube at 26 hpf; (*E*) the somites and mesenchyme of the fin buds (arrows); and (*F*) the facial, jaw, and pectoral fin muscles at 72 hpf. (*G–K′*) Comparison of *SERCA2* expression in wild-type (*G–K*) and *tre* mutants (*G′–K′*). (*G* and *G′*) At 30 hpf, *SERCA2* expression in *tre* heart tubes is comparable to wild type. However, at (*H* and *H′*) 48 hpf, (*J* and *J′*) 53 and 72 hpf (not shown) wild-type embryos show diffuse expression of *SERCA2* in the atrium, whereas *tre* mutants show robust expression of *SERCA2* in the atrium. At (*I* and *I′*) 48 hpf and (*K* and *K′*) 53 and 72 hpf (not shown), probes for pancardiac genes *cmlc2* (and *tbx20*, not shown) exhibit the usual diffuse signal in the atrium for both wild-type and *tre* embryos, indicating robust expression of *SERCA2* in *tre* mutants is not an artifact of morphology. (*L–T*) *SERCA2* knockdown phenotypes. Embryos injected with 17 ng of (*M*, *P*, and *S*) *SERCA2* morpholino (MO2) or (*Q* and *T*) 5 μM CPA have heart rates ≈30–50% slower than normal. Hearts show weak contractility in both chambers and fail to loop but no fibrillation or arrhythmia (other than heart rate). Most fail to circulate blood. *SERCA2*-inhibited embryos are touch-insensitive although not completely paralyzed. a, atrium; v, ventricle.

tilization. Coinjection of MO2 with *in vitro* synthesized wild-type zebrafish *SERCA2* RNA attenuates the above phenotypes and confirms their specificity (Table 1). Thus, *SERCA2* and *NCX1h* functions are each essential for zebrafish heart formation and for viability, but their loss-of-function phenotypes are distinct.

The ability of *tre^{m139}* atrial cells to contract at all indicates that proteins other than NCX1h are capable of removing Ca^{2+} from the cytosol after contraction. No known Na$^+$/Ca^{2+} exchangers other than NCX1 have been shown to be active in cardiac myocytes (29).

It is conceivable that myocardial cells might maintain calcium homeostasis by increasing expression or activity of SERCA2. To determine whether *SERCA2* expression levels are altered in response to NCX1 deficiency in zebrafish, we examined *tre* mutants by *in situ* hybridization. We find no obvious difference in *SERCA2* expression levels in *tre* mutant hearts through 30 hpf, well after contractile abnormalities become evident (Fig. 4 *G* and *G′*). However, at later timepoints (Fig. 4 *H*, *H′*, *J*, and *J′*), *SERCA2* expression in the atrium of *tre* mutants appears markedly more
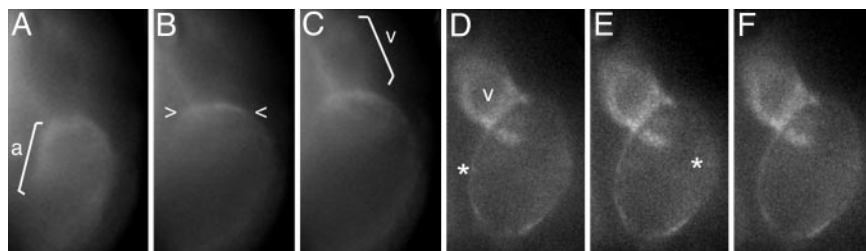

Fig. 5. *NCX1h* mutation leads to calcium overload in the *tre* ventricle. Analysis of intracellular calcium levels in 48 hpf embryos by calcium orange fluorescent dye. Selected sequential frames at ≈70-msec intervals are shown. (*A–D*) In wild-type embryos, Ca^{2+} entry into cardiomyocytes, denoted by dye, sweeps across the heart in a wave (brackets) correlated with the sequential contraction of the chambers. (*E–H*) In *tre* mutants, calcium orange levels in the ventricle remain static and appear elevated relative to the atrium, suggesting calcium overload in the ventricle. Calcium signals corresponding to one or a few adjoining cells briefly fluoresce in the fibrillating atrium (see faint signals to right of *). Image is anterior to the top. a, atrium; v, ventricle.

www.manaraa.com

robust than in wild type. In contrast, *in situ* hybridization using two pancardiac markers (Fig. 4 *I, I′, K, K′* and data not shown) gives similar patterns of expression in wild-type and *tre* hearts, indicating that the abnormal morphology of the *tre* atrium has not artificially "concentrated" the SERCA2 signal.

We next investigated the effects of loss of *NCX1h* or *SERCA2* activity on calcium handling in the early heart by tracking calcium levels in live embryos injected with calcium-sensitive fluorescent dye. In wild-type embryos, Ca^{2+} entry into cardiomyocytes occurs in a wave across the heart in a pattern consistent with sequential excitation of the atrium and ventricle (Fig. 5 *A–C*; see also Movie 5, which is published as supporting information on the PNAS web site). In contrast, calcium levels in the *tre* ventricle are static and appear elevated relative to the atrium (Fig. 5 *D–F*; see also Movie 6, which is published as supporting information on the PNAS web site), suggesting calcium overload occurs in this chamber. Fluorescent signals in the *tre* atrium were sporadic and unsynchronized, consistent with the fibrillating phenotype. In *SERCA2* morphants, waves of Ca^{2+} entry progressed at a rate reflecting the slower heart beat, but calcium overload did not occur (data not shown).

Previous work established that both NCX1 and SERCA2 are involved in extrusion of calcium from intracellular space (6, 7), yet we find these proteins play distinct roles in establishing early rhythm in the embryonic heart. Defects in NCX1h function prohibit the establishment of regular coordinated rhythm of cardiomyocytes in the forming heart. Homozygous *tre* mutant embryos display fibrillation and other arrhythmic phenotypes not noted in loss-of-function mouse models of NCX1 (13–15). Thus, the *tre* mutant provides a unique animal model for the study of origin or suppression of NCX1-based arrhythmias. Abrogation of NCX1h function in the early zebrafish heart leads to defects in calcium transients and creates calcium overload in the ventricle. Recent reports demonstrate that blocking calcium transients attenuates sarcomere assembly in cultured myocytes (30, 31), suggesting a related mechanism might underlie sarcomeric defects in *tre* hearts. In contrast to *tre* phenotypes, morpholino-mediated inhibition of SERCA2 in forming hearts did not lead to fibrillation but slowed heart rate and diminished contractility and growth in both chambers to the point of embryonic lethality. Collectively, our data demonstrate that inhibition of NCX1h versus SERCA2 activity differentially affects the pathophysiology of rhythm in the developing heart and suggest the relative levels of both calcium-handling proteins constitute an important aspect of normal development.

1. Moorman, A. F. & Christoffels, V. M. (2003) *Novartis Found. Symp.* **250,** 25–34; discussion 34–43, 276–279.
2. Stainier, D., Lee, R. & Fishman, M. (1993) *Development (Cambridge, U.K.)* **119,** 31–40.
3. Priori, S. G., Napolitano, C. & Vicentini, A. (2003) *J. Interv. Card. Electrophysiol.* **9,** 93–101.
4. Kimura, J., Noma, A. & Irisawa, H. (1986) *Nature* **319,** 596–597.
5. Reeves, J. & Hale, C. (1984) *J. Biol. Chem.* **259,** 733–739.
6. Bridge, J., Smolley, J. & Spitzer, K. (1990) *Science* **248,** 376–378.
7. MacLennan, D. (1970) *J. Biol. Chem.* **245,** 4508–4518.
8. Bers, D. (1991) *Ann. N.Y. Acad. Sci.* **639,** 375–385.
9. Reed, T., Babu, G., Ji, Y., Zilberman, A., Ver Heyen, M., Wuytack, F. & Periasamy, M. (2000) *J. Mol. Cell Cardiol.* **32,** 453–464.
10. Tohse, N., Seki, S., Kobayashi, T., Tsutsuura, M., Nagashima, M. & Yamada, Y. (2004) *Jpn. J. Physiol.* **54,** 1–6.
11. Luss, I., Boknik, P., Jones, L., Kirchhefer, U., Knapp, J., Linck, B., Luss, H., Meissner, A., Muller, F., Schmitz, W., *et al.* (1999) *J. Mol. Cell Cardiol.* **31,** 1299–1314.
12. Cho, C., Kim, S., Jeong, M., Lee, C. & Shin, H. (2000) *Mol. Cells* **10,** 712–722.
13. Wakimoto, K., Kobayashi, K., Kuro-O, M., Yao, A., Iwamoto, T., Yanaka, N., Kita, S., Nishida, A., Azuma, S., Toyoda, Y., *et al.* (2000) *J. Biol. Chem.* **275,** 36991–36998.
14. Koushik, S., Wang, J., Rogers, R., Moskophidis, D., Lambert, N., Creazzo, T. & Conway, S. (2001) *FASEB J.* **15,** 1209–1211.
15. Cho, C. H., Kim, S. S., Jeong, M. J., Lee, C. O. & Shin, H. S. (2000) *Mol. Cells* **10,** 712–722.
16. Linask, K., Han, M., Artman, M. & Ludwig, C. (2001) *Dev. Dyn.* **221,** 249–264.
17. Nicoll, D., Ottolia, M. & Philipson, K. (2002) *Ann. N.Y. Acad. Sci.* **976,** 11–18.
18. Nicoll, D., Hryshko, L., Matsuoka, S., Frank, J. & Philipson, K. (1996) *J. Biol. Chem.* **271,** 13385–13391.
19. Ottolia, M., John, S., Qiu, Z. & Philipson, K. (2001) *J. Biol. Chem.* **276,** 19603–19609.
20. Yelon, D., Horne, S. & Stainier, D. (1999) *Dev. Biol.* **214,** 23–27.
21. Wakimoto, K., Kuro-o, M., Yanaka, N., Komuro, I., Nabeshima, Y. & Imai, Y. (2001) *Comp. Biochem. Physiol. B* **130,** 191–198.
22. Garrity, D., Childs, S. & Fishman, M. (2002) *Development (Cambridge, U.K.)* **129,** 4635–4645.
23. Yelon, D., Ticho, B., Halpern, M., Ruvinsky, I., Ho, R., Silver, L. & Stainier, D. (2000) *Development (Cambridge, U.K.)* **127,** 2573–2582.
24. Rottbauer, W., Baker, K., Wo, Z., Mohideen, M., Cantiello, H. & Fishman, M. (2001) *Dev. Cell.* **1,** 265–275.
25. Guerini, D., Guidi, F. & Carafoli, E. (2002) *FASEB J.* **16,** 519–528.
26. Yard, N., Chiesi, M. & Ball, H. (1994) *Br. J. Pharmacol.* **113,** 1001–1007.
27. Takahashi, S., Kato, Y., Adachi, M., Agata, N., Tanaka, H. & Shigenobu, K. (1995) *J. Pharmacol. Exp. Ther.* **272,** 1095–1100.
28. Creton, R. (2004) *Brain Res. Dev. Brain Res.* **151(1–2),** 33–41.
29. Henderson, S. A., Goldhaber, J. I., So, J. M., Han, T., Motter, C., Ngo, A., Chantawansri, C., Ritter, M. R., Friedlander, M., Nicoll, D. A., *et al.* (2004) *Circ. Res.* **95,** 604–611.
30. Harris, B. N., Li, H., Terry, M. & Ferrari, M. B. (2005) *Cell Motil. Cytoskeleton* **60,** 129–139.
31. Li, H., Cook, J. D., Terry, M., Spitzer, N. C. & Ferrari, M. B. (2004) *Dev. Dyn.* **229,** 231–242.
32. Langenbacher, A. D., Dong, Y., Shu, X., Choi, J., Nicoll, D. A., Goldhaber, J. I., Philipson, K. D. & Chen, J.-N. (2005) *Proc. Natl. Acad. Sci. USA* **102,** 17699–17704.
33. Schwarz, E. M. & Benzer, S. (1997) *Proc. Natl. Acad. Sci. USA* **94,** 10249–10254.
34. Levitsky, D., Nicoll, D. & Philipson, K. (1994) *J. Biol. Chem.* **269,** 22847–22852.
35. Matsuoka, S., Nicoll, D., Hryshko, L., Levitsky, D., Weiss, J. & Philipson, K. (1995) *J. Gen. Physiol.* **105,** 403–420.